Indian Journal of Pure & Applied Physics
Vol. 55, February 2017, pp. 135-144

Conceptual design of a thermal neutron radiography facility in the cyclotron 30 LC using the MCNPX code

Ismail Shaaban*

Nuclear Engineering Department, Atomic Energy Commission, Damascus 6091, Syria

Received 3 January 2016; revised 13 December 2016; accepted 29 December 2016

The MCNPX code and the ENDF/B-VII cross-section library have been used to optimize the geometrical dimensions of the thermal neutron radiography facility (TNRF) based on the cyclotron 30 LC using a Be target as a neutron source and the Protons Beam Channel (PBC) with energy 15.0 MeV and 20.0 MeV. Thermal, epithermal and fast neutron energy ranges have been selected as < 0.4 eV, 0.4 eV–10 keV and >10 keV, respectively. The calculated values of the thermal neutron flux at the main collimator exit (MCE) have been estimated to be 1.31×10^5 n/cm^2.s and 1.05×10^5 n/cm^2.s, 1.97×10^5 n/cm^2.s and 1.66×10^5 n/cm^2.s for the ratio L/D = 90 and L/D = 110, and the PBC with energy 15.0 MeV and 20.0 MeV, respectively. In addition, the cooling system of the Be target has been designed using solid works program. The simulated results showed that the maximum temperature of the Be target is lower than the melting temperature of the Be target. The use of neutronic and gamma filters has been eliminated in the design phase reducing the economic cost had anyone thought to build this beam.

Keywords: Neutron radiography, Cyclotron, MCNPX code, Thermal neutron flux, Be target

1 Introduction

Neutron radiography (NR) is a technique for visualizing the structure of an object by measuring the neutron flux passing through this object in two dimensions. As neutrons interact with matter in a different way than gamma and X-rays, the resulting radiographs are also different. Neutron radiography can therefore be used as a complementary inspection method to X-ray and gamma radiography[1,2]. The X-ray attenuation increases with higher electron density, whereas the neutrons are attenuated by light materials for example: hydrogen, boron and lithium, because they interact with the nuclei[1,2]. The NR is therefore, employed in a wide range of investigations such as test of the nuclear fuel rods and turbine blades, materials science and industrial products, hydrogen diffusion in metals, investigation of works of art, biological and plant physiological research[1-6].

Neutron radiography sources are available in three general types: radioisotopes, nuclear reactors and accelerators[4-9]. In this paper, the Syrian cyclotron 30 LC was used as a source to design the TNRF using the MCNPX code and the ENDF/B-VII cross - section library. In particular, the Be target as a neutron source and the PBC with energy 15.0 MeV and 20.0 MeV were used in this design. To reduce the economic cost of the TNRF had anyone thought to build this beam in the Syrian cyclotron 30 LC; a new design is being proposed. This design depends on the change of the neutronic beam direction coming from the neutron source to eliminate the use of the neutronic and gamma filters[1,10,11].

*E-mail: pscientific3@aec.org.sy

2 Material and Methods

2.1 The Syrian protons cyclotron

The cyclotron 30 LC is of the type cyclotron-30 LC. The main specifications of this cyclotron are given in Table 1. In this work, the energy of protons made in this cyclotron is fixed at 15.0 MeV and 20.0 MeV while the proton current on the target runs up to 200.0 μA.

2.2 Selection of the target material

The Be target is chosen as a neutron source, because it has the highest neutron yield and the smallest gamma ray yield per neutron. Further, Be has the highest thermal conductivity and a high melting point as shown in Table 2. As well as, a Be target is directly cooled by pure compressed water and the nuclei produced in a Be target have lower activity[12-14].

2.3 Comparison of the neutron spectrum of the ^{9}Be(p,n)^{9}B and ^{207}Pb(p,n) calculated with MCNPX code with the reference values

The unavailability of data about neutron and gamma ray yield of the ^{9}Be(p,n)^{9}B reaction for the

PBC with energy 15.0 MeV or 20.0 MeV induced to validate the calculation model adopted in this paper for other energy ranges to enable comparing results with published data. The neutron yield of the ^{9}Be(p,n)^{9}B reaction was calculated using protons with energy from 2.0 to 7.0 MeV and compared with the reference calculated and experimental values. In addition to that the neutron yield of the ^{207}Pb(p,n) reaction was calculated using protons with energy from 10.0 to 75.0 MeV and compared with published experimental values. The neutron yield of the ^{9}Be(p,n)^{9}B and ^{207}Pb(p,n) was calculated as follows: (i) The Be and Pb target with area = 2.50 cm^{2} and 0.50 cm thickness, and with 2.50 diameter and 2.50 cm thickness as described in references[15,16], respectively, were described using the SDEF card[17]. The Be and Pb target were placed in the center of spheres from air with 5.0 cm radius and bombarded at an angle of 0^{0} by (2.0 – 7.0) MeV and (10.0 – 75.0) MeV protons, respectively.

The F2 tally[17] was used to calculate the neutrons yield of the ^{9}Be(p,n)^{9}B and ^{207}Pb(p,n) reaction. The calculated values besides to other calculated and experimental results belonging to a group of researchers are shown in Figs 1 and 2. As a results from Figs 1 and 2 there is a good agreement between calculated values and the results of the references[15,16] with an error not exceeding 2.24% for the Be target and less than the 1.0% for the Pb target. The good agreement between the calculated values using the MCNPX code and the reference values for the neutrons yield of the ^{9}Be(p,n)^{9}B and ^{207}Pb(p,n) reactions were used as reference for designing TNRF in the cyclotron 30 LC.

Table 1 — Main specifications of the cyclotron 30 LC

Energy of protons	(15.0 – 30.0) MeV
Protons current	200.0 μA
Simultaneous extracted beam	2.0
External beam line	2.0 m to 6.0 m
Hill field	1.70 Tesla
Valley field	0.12 Tesla
Coils D.C. power	8.0 kW
Frequency	65.0 MHz
Power	25.0 kW
Injection H^{-} current	5.0 mA
Cyclotron vault dimension	8.0 × 7.5 × 4.0 m
Total weight	50.0 tons

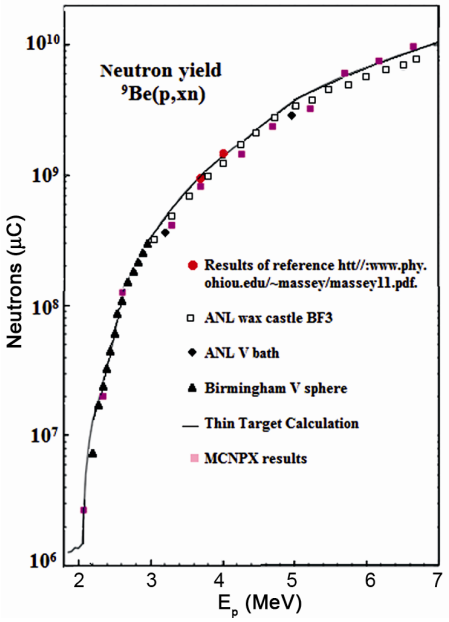

Fig. 1 — The calculated and experimental values of the neutrons spectrum emission from Be target bombarded by (2.0 – 7.0) MeV protons

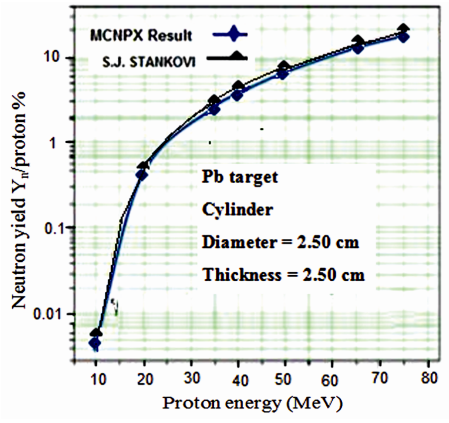

Fig. 2 — The calculated and experimental values of the neutrons spectrum emission from Pb target bombarded by (10.0 – 75.0) MeV protons

Table 2 — Target material property compared with Li, Be, Ta and W

Melting point (°C)	Boiling point (°C)	Thermal conductivity (W/m-K)	Neutron yield (s/mA)	Gamma-ray yield (s/mA)	Gamma ray yield per one neutron
180	1340	84.7	1.14E+14	9.80E+12	0.09
1278	2970	201	1.90E+14	3.35E+12	0.02
3017	5458	57.5	1.27E+14	1.18E+14	0.93
3422	5555	174	9.65E+13	1.35E+14	1.40

2.4 Coolant system of Be target

The deposited power in the Be target material is 3.0 kW and 4.0 kW for the PBC 15.0 MeV and 20.0 MeV, respectively. This power heats the target to a high temperature enough to melt it. Therefore, a cooling system was designed for the Be target to be cooled and prevented from melting. The coolant system consists of two concentric copper tubes with 10.0 cm in length. The diameters of the outer and inner copper tubes are 2.0 cm and 1.0 cm, respectively. The thickness of these tubes is 0.10 cm as shown in Fig. 3.

The solid works program was used to calculate the variation of the Be target temperature as a function of the cooling flow rate, where the following parameters were taken in the simulation as light water as a coolant, initial temperature of water is 20 °C (T_{inlet} = 20 °C) and pressure is 1 atm, copper material as a heat exchanger between Be target and coolant, Be target as a heat source equivalent to 3.0 kW and 4.0 kW, dimensions of the target are 0.50 cm radius and 0.30 cm thickness.

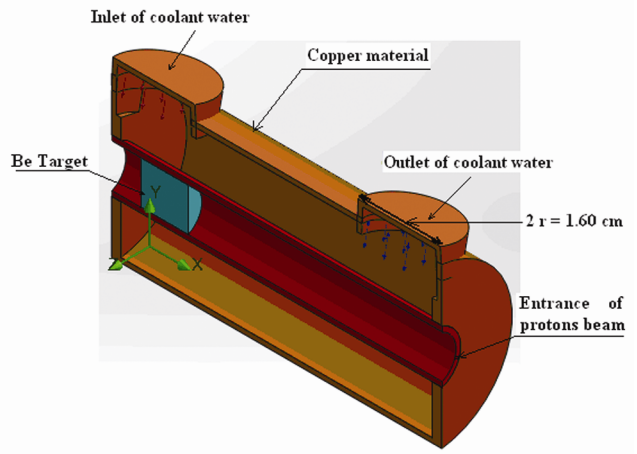

Fig. 3 — 3-D view of the cooling system of the Be target using the solid works program

The simulated results are given in Table 3 where T_{Be} (K) is the Be target temperature, T_{H2O} (K) is the coolant water temperature at exit , ΔP (kPa) is the pressure difference for a given fluid, m (kg/s) is the flow rate of the cooling water, V_{H2O} (m/s) is the velocity of the cooling water flow. From Table 3 the maximum temperature of the Be target with cooling water is T_{max} (K) = 673 K and 791 K for the PBC with energy 15.0 MeV and 20.0 MeV, respectively. This temperature is smaller than the melting temperature of the Be target as shown in Table 2.

Figure 4 shows the distribution of the heat in the Be target material using the solid works program. In

Table 3 — Variation of the Be target and cooling water temperature, velocity of the cooling water and the difference of the pressure as a function of the flow rate of the cooling water for the PBC with energy 15.0 MeV and 20.0 MeV

M (kg/s)	T_{Be} (K)	T_{H2O} (K)	V_{max}(m/s)	ΔP (kPa)
Energy of protons beam = 15.0 MeV				
0.5	673	331	2.4	6660
1	579	321	4.7	26578
1.5	526	315	7.2	62653
2	478	312	9.4	112084
2.5	462	308	16	174367
3	449	306	8	244289
Energy of protons beam = 20.0 MeV				
0.5	791	343	2.3	118625
1	659	329	4.7	61467
1.5	560	321	6.9	696
2	525	317	9	109036
2.5	510	314	11.5	135671
3	493	312	13	243654

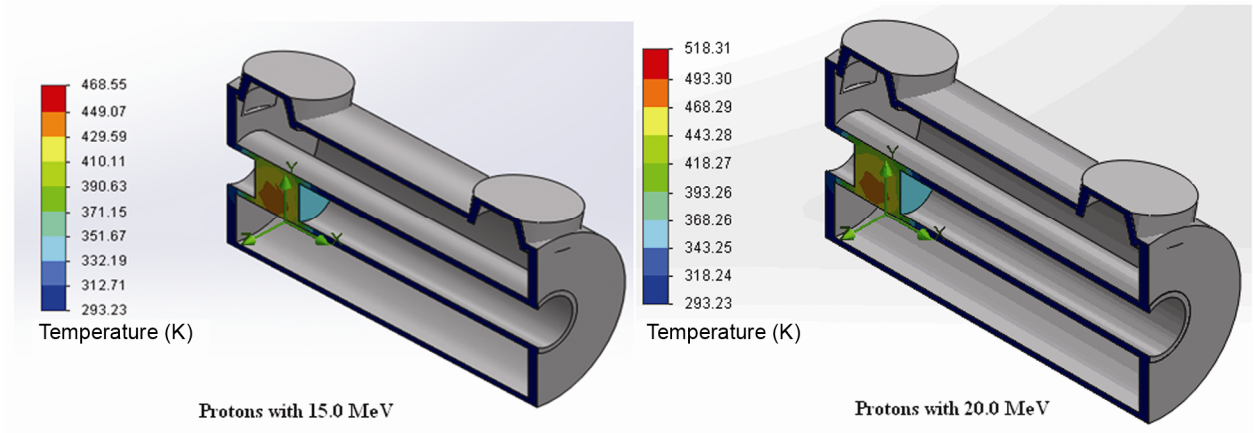

Fig. 4 — Variation of the Be target temperature for the PBC with energy 15.0 MeV and 20.0 MeV using the solid works program

addition, Figs 5 and 6 show the simulation results by solid works program of the variation of the velocity and pressure of the cooling water in the outer tube around the Be target at the value 2.50 kg/s, respectively.

3 Optimization of Geometrical Dimensions of TNRF in Cyclotron 30 LC using MCNPX Code

The TNRF consists of the neutron source, neutron reflector, lead for gamma ray, neutron collimator.

3.1 Neutron source

The neutron source consists of the Be target with 0.30 cm thickness and 0.50 cm radius. The Be target was placed inside the aluminum tube with 0.50 cm radius, and located at distance 36.0 cm from the edge of the aluminum tube as shown in Figs 7, 8 and 9. The Be target was surrounded with the cooling system while the aluminum tube was used to direct the protons beam to the Be target.

3.2 Neutron reflector

The Be target was surrounded with beryllium and graphite reflectors to prevent the neutrons from escaping to the environment, reduce the leakage of the neutrons and to direct them to the primary collimator of the neutrons as shown in Figs 7, 8 and 9.

The neutron reflector consists of two parts: the first part consists of the beryllium cylinder with diameter 44.0 cm and 32.0 height. This part surrounds the Be target (neutron source), a part of the aluminum tube and coolant system as shown in Figs 7, 8 and 9. And the second part consists of the graphite cylinder with 100.0 cm diameter and 59.0 cm height as shown in Figs 7, 8 and 9. This part surrounds the beryllium reflector, a part of coolant system and is placed inside the cylinder made of stainless steel with 100.1 cm diameter, 59.0 cm height and 1.0 cm thickness to absorb the neutrons and gamma rays.

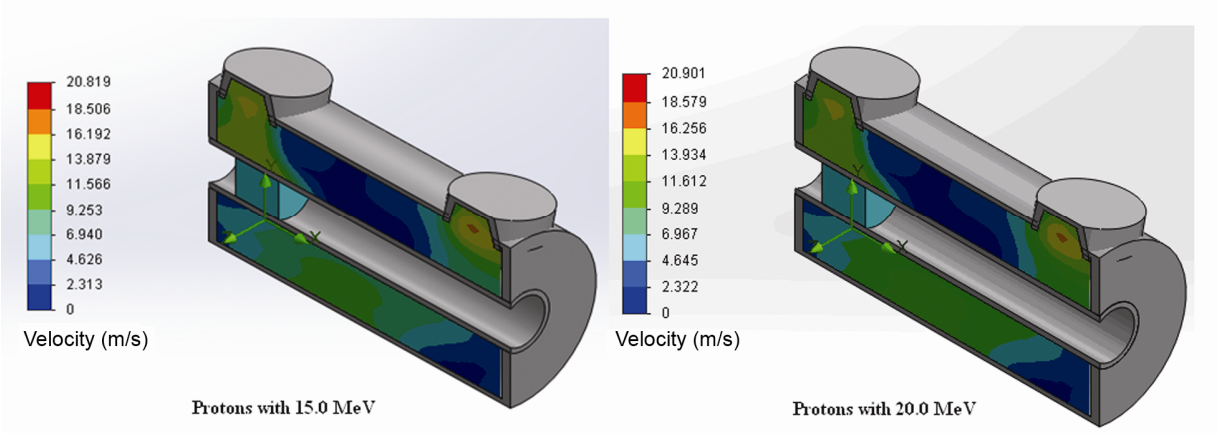

Fig. 5 — Variation of the coolant water velocity inside cooling tube for the PBC with energy 15.0 MeV and 20.0 MeV using the solid works program

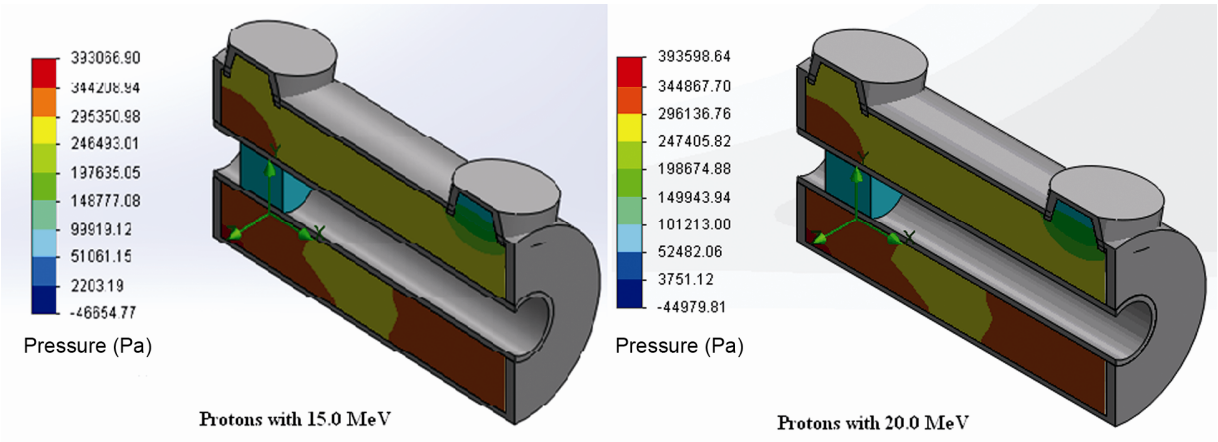

Fig. 6 — Variation the pressure of the coolant water inside cooling tube for the PBC with energy 15.0 MeV and 20.0 MeV using the solid works program

3.3 Lead for the gamma rays

The gamma ray forms as a result of the reaction between protons and neutrons with the Be target and the cooling system materials, respectively. This degrades the quality of the image of the studied sample. Therefore, to reduce the gamma ray dose at the MCE, a lead cylinder with diameter 80.0 cm, thickness 5.0 cm and 35.0 cm height was placed beyond the primary collimator of neutrons as shown in Figs 7, 8 and 9.

3.4 Collimator of neutrons

The collimator of neutron consists of two collimators: primary collimator; this collimator is a parallelpied with dimensions 2.50 cm width, 5.0 cm length and 22.0 cm height. This collimator is mounted inside the graphite cylinder with 80.0 cm diameter and 35.0 cm height as shown in Figs 7, 8 and 9.

The graphite was used to moderate the fast neutrons through the elastic and inelastic collisions and direct them to the neutronic aperture. The

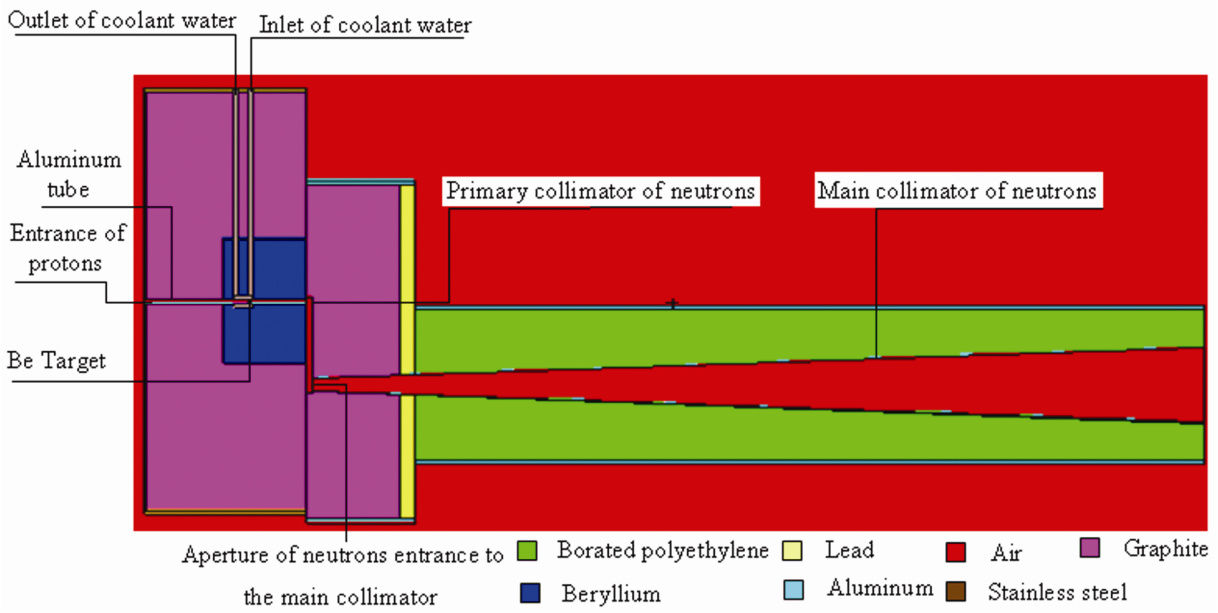

Fig. 7 — Vertical cross section of the TNRF in the cyclotron 30 LC using the MCNP5-beta code

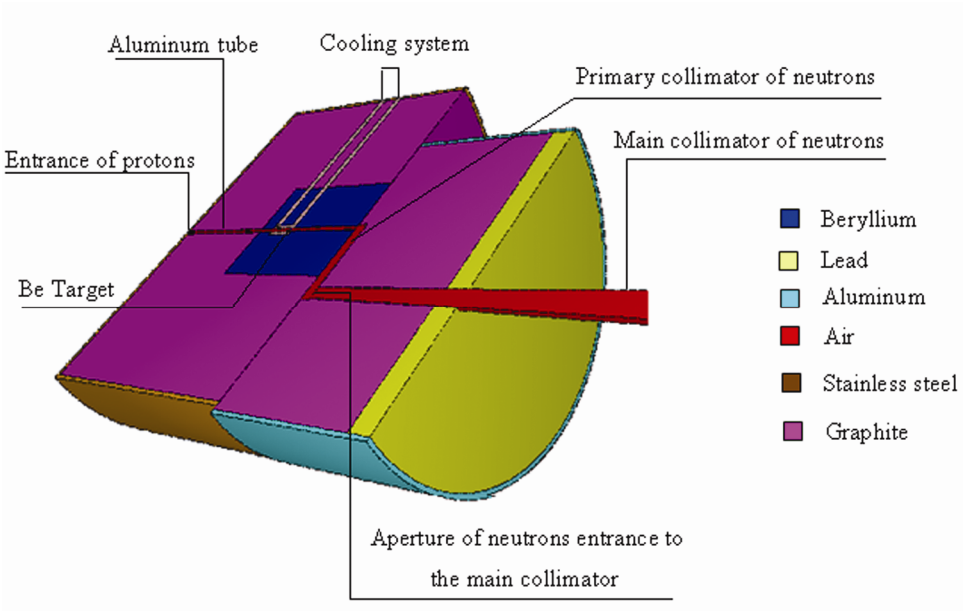

Fig. 8 — Horizontal cross section of the TNRF in the cyclotron 30 LC using the MCNP5-beta code

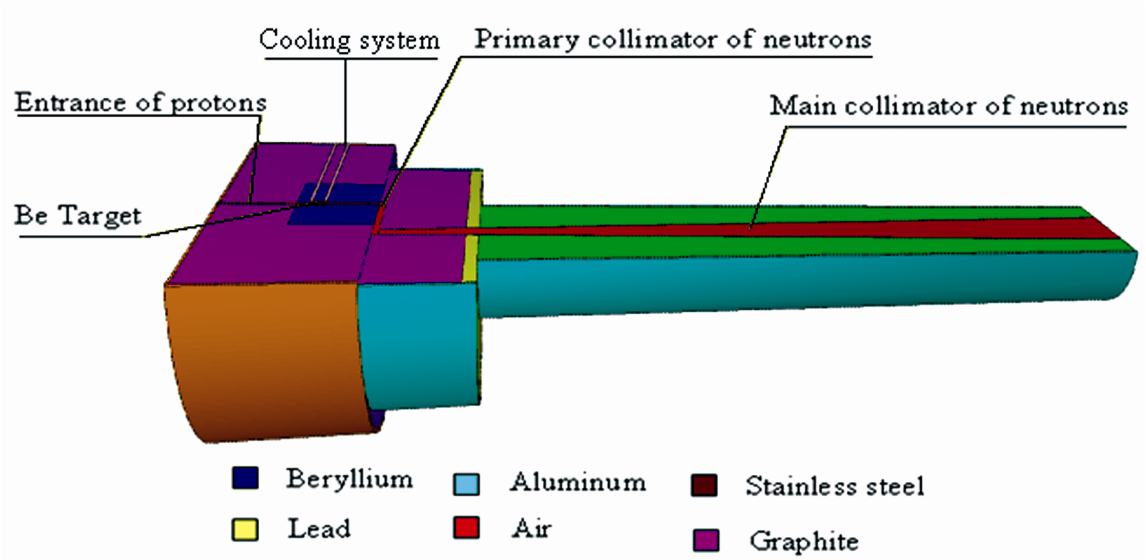

Fig. 9 — 3-D view of the TNRF in the cyclotron 30 LC using the MCNP5-beta code

primary collimator was designed perpendicular to the symmetry axis of the proton beam to make the fast neutrons lose a big part of their energy. The main collimator is defined as the distance from the aperture of the neutrons entrance to the beam exit and consists of the diverging cone section with a length 330.0 cm and 18.0 cm diameter of the beam exit. Where the divergent beam collimator is mainly used after the conclusion of Barton[11] in 1967 that divergent beam collimators produce highest resolution[1,5]. This collimator is mounted inside the aluminum cylinder with 36.0 cm diameter and 0.30 cm thickness of wall as shown in Figs 7 and 9. The walls of the main collimator are made of Al-6061 alloy with thickness 1.0 mm. The space between the walls of the aluminum cylinder and the diverging cone section is filled with borated polyethylene (5.0% Boron) to absorb the neutrons which form as a result of the reaction between neutrons and the TNRF materials. The geometrical dimensions of neutron reflectors, cooling system, site of the Be target, lead sheet and neutron collimator were optimized using the MCNPX code to have a high value of the thermal neutron flux and acceptable value of the gamma ray dose at the beam exit. In this optimization, the MCNPX code was run several times (600.000.000 particle histories were used each time) for both the L/D = 90 and L/D = 110 ratios (where L is the length of the main collimator and D is the diameter of the aperture of the neutrons entrance to the main collimator) and both the PBC with energy 15.0 MeV and 20.0 MeV.

4 Calculation of Thermal Neutron Flux and Gamma Ray Dose at MCE for PBC with Energy 15.0 MeV and 20.0 MeV

The SDEF card and tally F5: N P[17] was used to describe the neutron source (Be target) and to calculate the thermal (Φ_{ther}), epithermal (Φ_{epith}), fast (Φ_{fas}) neutron flux and gamma ray dose (D_γ) at the beam exit.

To calculate the Φ_{ther}, Φ_{epith}, Φ_{fas} and D_γ, the MCNPX code was run for the 600.000.000 particle histories with the 7.87×10^{12} n/s, 1.32×10^{13} n/s and 3.09×10^{11} p/s, 4.31×10^{11} p/s number of the neutrons and photons per second which emit from the Be target with 0.30 cm thickness and 0.50 cm radius for the PBC 15.0 MeV and 20.0 MeV, respectively. The number of neutrons and photons per second was calculated using the MCNPX code[17] as mentioned in section 2.3. The KERMA factors[17] in the calculation of the D_γ were used too.

The calculated values of the Φ_{ther}, Φ_{epith}, Φ_{fas} and D_γ with the cooling system are given in Table 4. The calculated values of the T_{H2O} (K) = 331 K and T_{Be} (K) = 673 K, T_{H2O} (K) = 343 K and T_{Be} (K) = 791 K for the PBC with energy 15.0 MeV and 20.0 MeV, respectively, were taken also in the calculation. Additionally, the values of the Φ_{ther}, Φ_{epith} and Φ_{fas} without cooling system are calculated and tabulated in Table 5.

In the calculation Φ_{ther}, Φ_{epith} and Φ_{fas} with and without a cooling system, the neutron flux was tallied for thermal (below 0.40 eV), epithermal (between 0.40 eV and 10.0 keV) and fast neutron flux (over

Table 4 — Neutronic characteristics of the TNRF in the cyclotron 30 LC at the MCE

Energy of protons beam	15 MeV		20 MeV	
L/D	90	110	90	110
D (cm)	3.6	3	3.6	3
Φ_{ther} (n/cm^2.s)	(1.31±0.01)×10^5	(1.05±0.01)×10^5	(1.97±0.01)×10^5	(1.66±0.01)×10^5
$\Phi_{epither}$ (n/cm^2.s)	(9.55±0.03)×10^3	(7.4±0.04)×10^3	(1.65±0.04)×10^4	(1.39±0.05)×10^4
Φ_{fast} (n/cm^2.s)	(3.52±0.04)×10^3	(2.7±0.05)×10^3	(7.36±0.05)×10^3	(5.22±0.05)×10^3
Φ_{ther}/D_γ (n/cm^2.mR)	2.39×10^8	2.38×10^8	2.01×10^8	1.91×10^8
TNC %	91	91	90	90
2θ (degree)	2.54	2.60	2.54	2.60

Table 5 — Calculated values of the Φ_{ther}, Φ_{epith} and Φ_{fas} at the MCE of the TNRF without cooling system

Energy of protons beam	15 MeV		20 MeV	
L/D	90	110	90	110
D (cm)	3.6	3	3.6	3
Φ_{ther} (n/cm^2.s)	(2.22±0.04)×10^5	(1.59±0.02)×10^5	(3.86±0.01)×10^5	(2.99±0.01)×10^5
$\Phi_{epither}$ (n/cm^2.s)	(2.86±0.06)×10^4	(1.96±0.06)×10^4	(5.42±0.02)×10^4	(4.17±0.02)×10^4
Φ_{fast} (n/cm^2.s)	(1.09±0.01)×10^4	(7.45±0.03)×10^3	(2.40±0.04)×10^3	(1.67±0.03)×10^4

10.0 keV). Figures 10, 11, 12 and 13 show the distribution of the thermal neutron flux along the *Z* and *Y*–axis at the MCE of the TNRF.

5 Results and Discussion

The geometrical dimensions of the TNRF were optimized using the MCNPX code to have a high value of the Φ_{ther} (>10^5 n/cm^2.s) and thermal neutron content (TNC) > 90.0 % at the MCE for the PBC with energy 15.0 MeV and 20.0 MeV. These values ensure that the image of the sample being studied arise essentially from the thermal neutrons. This leads to enhance the contrast in the images of the isotopes of an element[1].

The value of the TNC is defined as the ratio of Φ_{ther} below 0.40 eV to the total neutrons flux in the range (0-20) MeV. From Table 4, it results that the calculated values of the ratio Φ_{ther}/D_γ for the PBC with energy 15.0 MeV and 20.0 MeV are in agreement with the condition $\Phi_{ther}/D_\gamma \geq 1.0\times10^6$ n/cm^2.mR[1,10]. This condition ensures that the gamma ray contribution to the generation of the image will be smaller than that coming from the thermal neutrons. The characteristics of the MC of neutrons such as: *D*, *L* and *L*/*D* ratio have a big effect on the image quality relating of the geometric unsharpness and the divergence angle of the beam. Where these parameters are determined as explained below: The geometric unsharpness U_g is determined by the formula[10]:

$$U_g = D\times t/(L-t) \quad \ldots (1)$$

where U_g is the geometric unsharpness, *t* is the object thickness, *D* is the diameter of the neutronic aperture, *L* is the distance from the aperture to the MCE. As a result from Eq. (1), the design of the neutronic beam with high value of the *L*/*D* ratio is more effective than the case when the *L/D* ratio is smaller. This leads to a less distorted image at the periphery of the studied sample[10]. Therefore, the *L* was taken 324 and 330 cm for *L*/*D* ratio 90 and 110, respectively. This leads to a less distorted image at the periphery of the studied sample the divergence angle of the beam is determined by the following equation[10]:

$$\tan\theta = 0.5(R-D)/L \quad \ldots (2)$$

where, θ is the half of the beam divergence angle, *R* is the diameter of the beam exit or MCE and equal to 18.0 cm, *L* is the distance from the source to the MCE, *D* is the diameter of the neutronic aperture.

From the Eq. (2), if the neutron beam diverges very rapidly (*L* is small) to a large size then the outer portion of the images produced will suffer significant distortion. Conversely, if the length of the main collimator of neutrons is long or the image size is small then the outer portion of the image will be less distorted[10]. Therefore it can be seen in Table 4 that the calculated value of the angle of the first and second neutronic beam divergence is equal to 2θ = 2.54 and 2.60° for the first and second neutronic beam, respectively. This lead to a homogeneous distribution of the thermal neutrons at the MCE (Figs 10, 11, 12 and 13). Therefore, the image of the studied sample will be less distorted and this image will have good contrast.

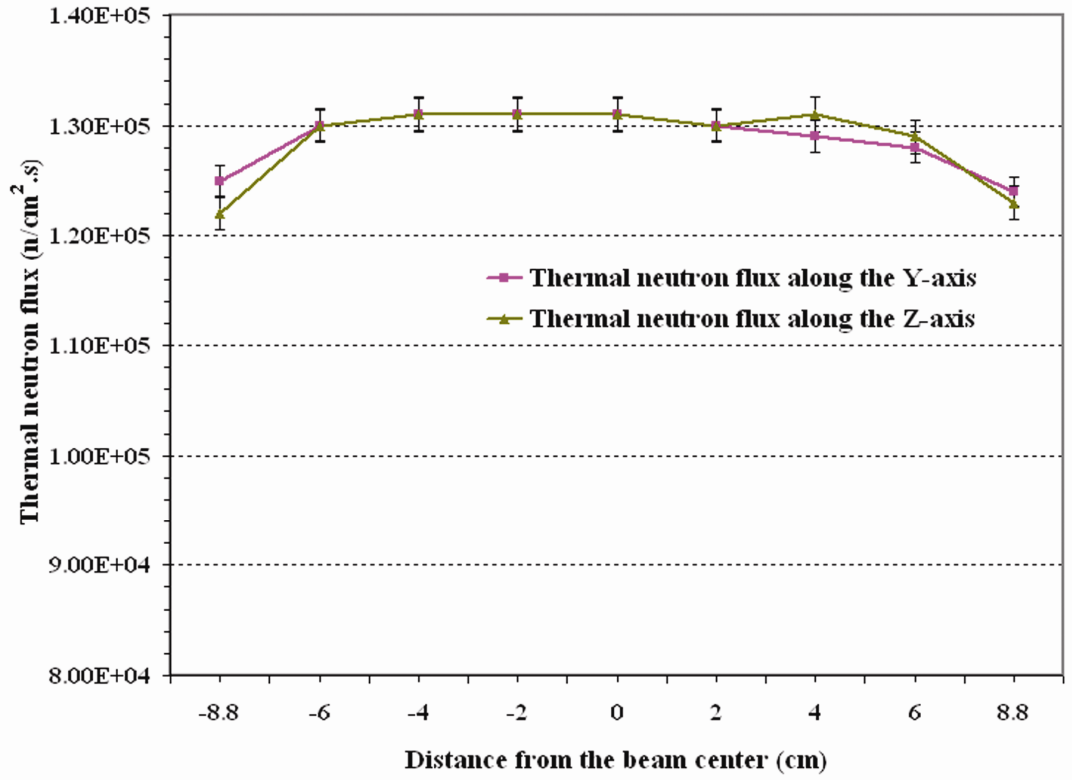

Fig. 10 — Distribution of the Φ_{ther} along the Z and Y- axis at the MCE of the TNRF for the PBC with energy 15.0 MeV and L/D = 90.0

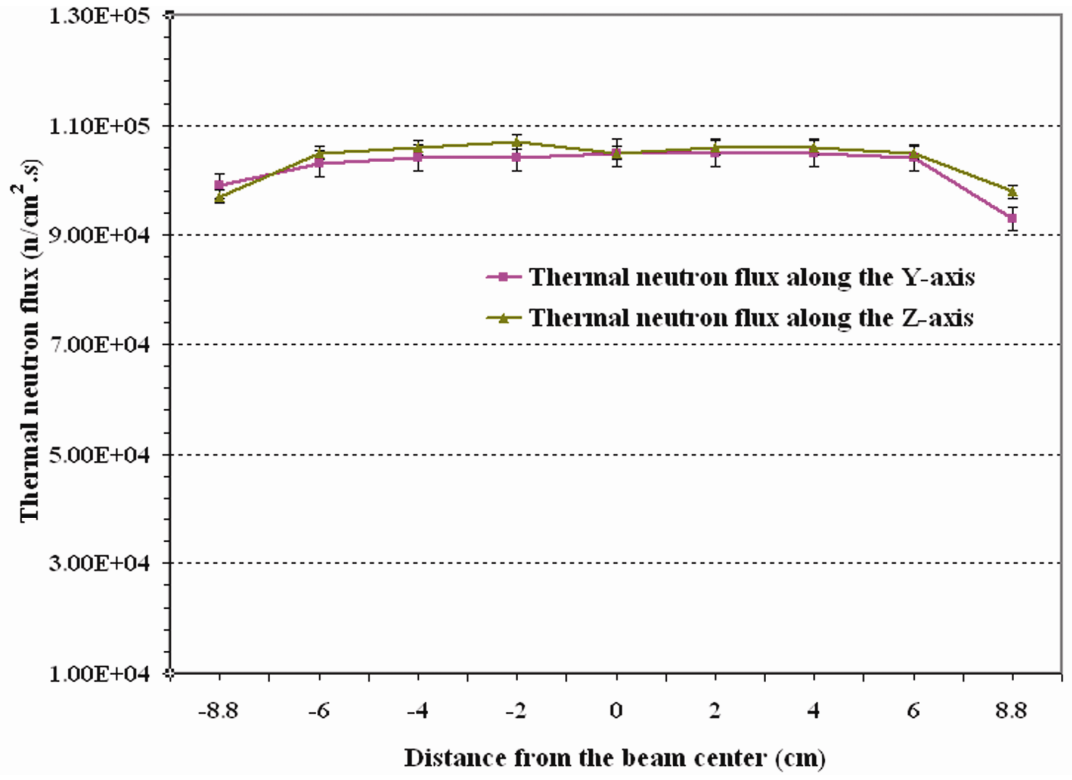

Fig. 11 — Distribution of the Φ_{ther} along the Z and Y- axis at the MCE of the TNRF for the PBC with energy 15.0 MeV and L/D = 110.0

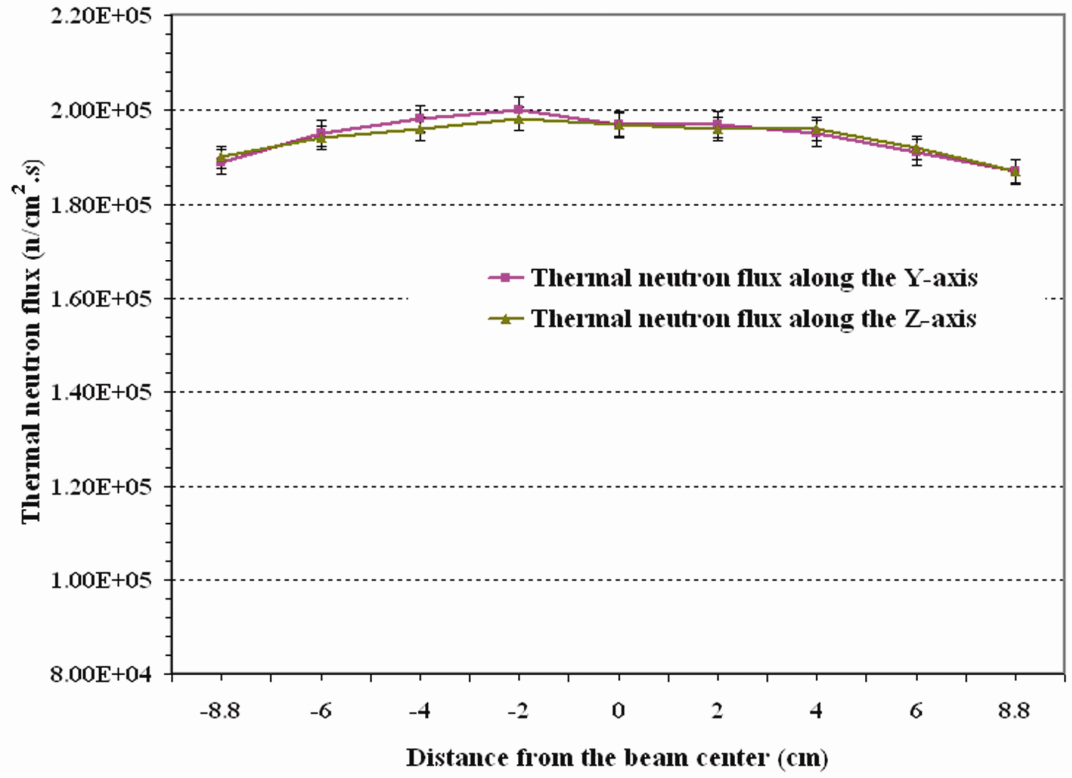

Fig. 12 — Distribution of the Φ_{ther} along the Z and Y- axis at the MCE of the TNRF for the PBC with energy 20.0 MeV and L/D = 90.0

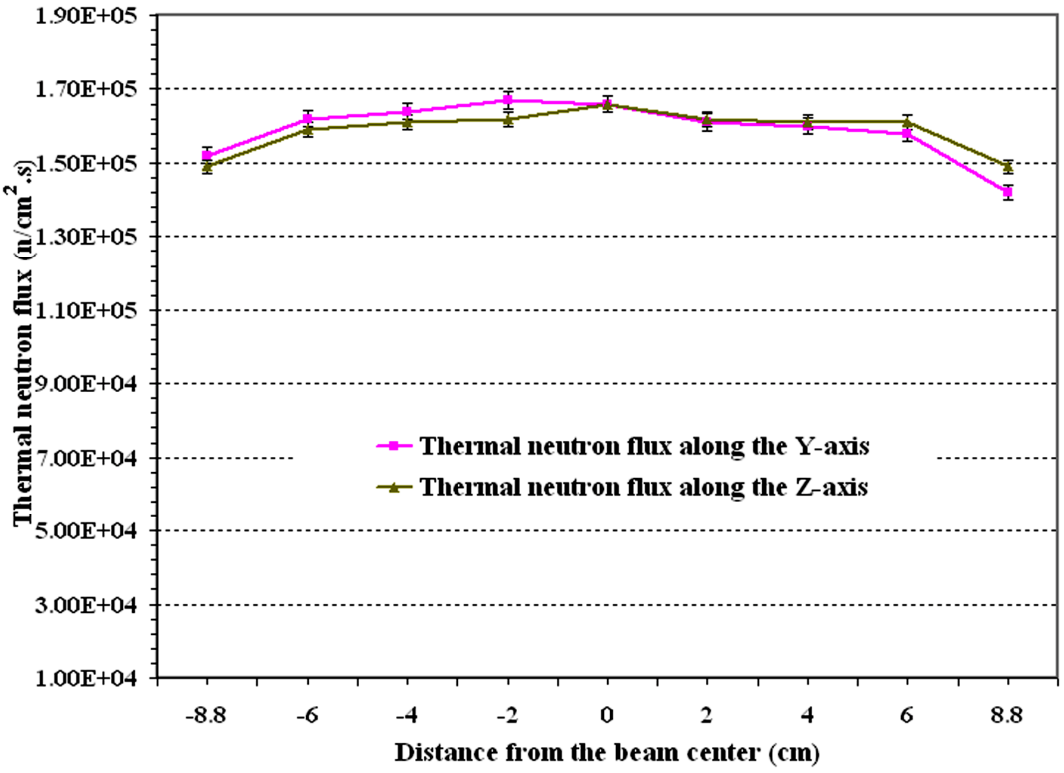

Fig. 13 — Distribution of the Φ_{ther} along the Z and Y- axis at the MCE of the TNRF for the PBC with energy 20.0 MeV and L/D = 110.0

Table 5 shows that the cooling system plays a very important role in the determination of the values Φ_{ther}, Φ_{epith} and Φ_{fas} at the MCE, where the differences between the values Φ_{ther}, Φ_{epith} and Φ_{fas} with the cooling system and the same values without the cooling system are 41%, 66% and 66%, 49%, 69% and 69% for the PBC with energy 15.0 MeV and 20.0 MeV, and L/D=90, respectively, and 34%, 62% and 64%, 44%, 67% and 68% for the PBC with energy 15.0 MeV and 20.0 MeV, and L/D=110, respectively. Theses differences come out because of the moderation of the epithermal and the fast neutrons by the surrounding water of the Be target where a big part of epithermal and fast neutrons loose them energy before reaching the MCE as thermal neutrons.

Figures 10, 11, 12 and 13 show the distribution of the thermal neutrons flux along the Z and Y - axis at the MCE for L/D = 90, 110 and PBC with energy 15.0 MeV and 20.0 MeV. It results from these figures that there is a good agreement between the calculated values and the maximum difference between them is 1.30 % and 1.84%, 1.55% and 1.90% for the ratio L/D = 90, 110 and PBC with energy 15.0 MeV and 20.0 MeV, respectively. Evidently, the calculated values of the thermal neutron flux for the ratio L/D = 90 are more homogeneous than the calculated values of the thermal neutron flux for the ratio L/D = 110. Here, the homogeneity between these values plays a very important role for getting clear image of the internal compostion of the studied sample especially for the isotopes of an element.

From Table 4 the calculated value of the raio TNC for the PBC with energy 15.0 MeV is higher than the calculated value for the PBC with energy 20.0 MeV. This result ensures that the designed neutronic beam using the PBC with energy 15.0 MeV is better than the designed neutronic beam using the PBC with energy 20.0 MeV. In this research the neutronic and gamma filters were not used as usual in the design of the neutronic beams. This reduces the economic cost to build this beam.

6 Conclusions

The geometrical dimensions of the TNRF in the Syrian cyclotron 30 LC and the neutron source (Be target) characteristics were optimized using the MCNPX code for the PBC with energy 15.0 MeV and 20.0 MeV and proton current equal to 200.0 μA. The results showed that the cyclotron 30 LC produces protons with energies large enough to produce neutrons with appropriate energy and flux for the TNRF and it does not require significant changes in design to provide these neutrons. In this design the beam filters (gamma and fast neutrons required for standard TNRF designs) were removed.

Acknowledgment

The author thanks Professor I Othman, Director General of Atomic Energy Commission of Syria, for his encouragement and continued support.

References

1 Kaushal K M, *Development of a thermal neutron imaging at the N.C.S.U PULSTAR Reactor*, Ph D thesis, North Carolina State University, 2005.
2 Thomas R C, *Development of neutron radioscopy at the SLOWPOKE-2 facility at RMC for the inspection of CF188 flight control surfaces*, Master of Engineering Thesis, Chemical and Materials, Faculty of the Royal Military College of Canada, 2000.
3 Puffer D B, *Moderator design for accelerator based neutron radiography and tomography systems*, Master of Science Thesis, Nuclear Engineering at Massachusetts Institute of Technology, 1994.
4 Zou Y, Wen W & Guo Z, *Nucl Instr Meth Phys Res A*, 651 (2011) 62.
5 Berger H & Iddings F, *Neutron radiography, Repot NTIAC-SR-98-01*, Louisiana State University, 1998.
6 Kǫrner S, Pleinert H, Bǫck H, *Review of neutron radiography activities atthe atominstitut of the Austrian Universities. In*: Proceedings of the 5th World Conference on Neutron Radiography, Berlin, 1996.
7 Shaaban I, *Ann Nucl Energy*, 37 (2010) 1588.
8 Matsumoto T, *Nucl Instr Meth Phys Res A*, 377 (1996) 48.
9 Mishra K K, Hawari A I & Gillette V H, *IEEE Trans Nucl Sci*, 53 (2006) 3904.
10 Shaaban I, *J Radioanal Nucl Chem*, 41 (2014) 301.
11 Barton J P, *J Non-destruct Test Eval*, 16 (2001) 95.
12 Blue T E & Yanch J C, *J Neuro-Oncology*, 62 (2003) 19.
13 Tanaka H, Sakurai Y & Suzuki M, *Nucl Instr Meth Phys Res B*, 267 (2009) 1970.
14 Yonai S, Itogaa T & Babaa M, *Appl Radiat Isot*, 61 (2004) 997.
15 Howard W B, Grimes S M, Massey T N, Al-Quraishi S I, Jacobs D K & Brien C E, Yanch J C, *Nucl Sci Eng*, 138 (2001) 145.
16 Stankovic S J, Ilic R D, Pesic M P & Marinkovic P M, *Neutron emission spectra calculated for proton beams from 10 MeV to 75 MeV at lead target*, Institute of Nuclear Sciences VINCA, Belgrade, Yugoslavia; Belgrade (Yugoslavia), 2001
17 Briesmeiste J F, *A General Monte Carlo N-Particle transport code Version 4C, LA-7396-M*, LosAlamos National Laboratory, New Mexico, USA, 1997.